NERC GEF Loans 846 (July-August 2007) & 866 (March 2008)

Hydraulic forcing of subglacial sediment properties and impact on glacier dynamics

- Final Report by Dr. Bernd Kulessa, 17th April 2009 -

School of the Environment and Society, Swansea University, Swansea SA2 8PP, UK,
b.kulessa@swansea.ac.uk, Tel. 01792-513163

Abstract

We demonstrate that temporally coincident collection and joint interpretation of high-quality differential GPS (supported by two consecutive GEF loans of four Leica 1200 receivers, which form the basis of this report), repeat seismic amplitude-versus-offset (AVO) and continuous ground-penetrating radar (GPR) data is well suited to characterising the spatiotemporal dynamics of the subglacial processes controlling the flow instability of the Grubengletscher, Valais, Switzerland. We find that basal motion of the Grubengletscher occurs principally by subglacial sediment deformation during much of the day in summer, although hydrologically-induced sliding events are common in the afternoon. The highest glacier flow velocities occur during these sliding events, as opposed to those measured during times of sediment deformation which are relatively slow and invariable. We conclude that hydrological processes are a governing control on basal mechanical processes at the Grubengletscher during the summer. More generally our study demonstrates that an integrated geophysical approach is well suited not only to characterising at a snapshot in time coupled hydrological and mechanical properties of the glacier bed, but also to monitoring changes in those properties over time. From this fundamental glaciological processes can be inferred, which may well hold true at outlet glaciers from Polar ice masses as they do for the Grubengletscher as a possible small-scale analogue.

1. Introduction

The Intergovernmental Panel on Climate Change (IPCC) predicts that sea level could rise by 0.5 ± 0.4 m by 2100[1]. The two principal contributions to this rise are thermal expansion of the oceans (up to 0.43 m) and freshwater influx (up to 0.34 m)[1]. Most influx is likely to come from the world's smaller ice caps and glaciers (up to 0.23 m) since these have shorter response times to climatic warming than the larger ice sheets. There are, however, at least two significant problems with the IPCC's predictions. First, the range of uncertainty (± 0.4 m) is unacceptably large given the significant socio-economic costs of such rise. Second, these predictions could underestimate considerably actual sea level rise since they are based almost exclusively on changes in the balance between ice mass melting and accumulation, ignoring ice dynamic effects[2,3]. To improve estimates of future sea level rise, inclusion of ice mass dynamics into predictive models of ice-climate-sea level interactions is an international research priority[2,4]. It has recently been hypothesized that surface melt waters can penetrate to the beds of outlet glaciers from larger ice sheets and ice caps[5-8], providing '… a clear mechanism for enhanced flow through basal lubrication and sliding…'[3]. This mechanism would represent an important link between climatic forcing, ice sheet or ice cap stability, and sea level rise. It is therefore urgent that this hypothesis is substantiated.

The terminal region of the Grubengletscher, Valais, Switzerland (Figure 1), flows at speeds of up to ~ 45 m year^{-1}, which is fast for an Alpine ice mass. This flow instability is due

almost entirely to basal mechanical processes[9], although the physical nature of these processes is poorly understood. Since the terminal region of the Grubengletscher rests on a thick layer of unlithified subglacial sediments[10], either sliding over or deformation of these sediments must sustain the instability. The coupled mechanical and hydrological processes operating at the base of the Grubengletscher could be a useful analogue for those facilitating the acceleration of outlet glaciers on [a] the Greenland Ice Sheet[11,12], which is predicted to be particularly sensitive to climatic warming[13]; and [b] the Antarctic Peninsula following the rapid retreat of the Larsen A and B ice shelves[14-17].

The principal aim of this project is to characterise the spatiotemporal dynamics of the subglacial processes controlling the flow instability using a combination of repeat acquisition of seismic Amplitude-Versus-Offset (AVO) data and automated ground-penetrating radar (GPR) and differential GPS-based monitoring of glacier velocity. The specific objectives are

[SO1] to identify whether subglacial sediment deformation or sliding is responsible for the flow instability;

[SO2] to characterise the impact of spatiotemporal changes in subglacial mechanical conditions on glacier flow velocity; and

[SO3] to identify whether the subglacial mechanical processes can be forced hydrologically.

The GEF loans which facilitated the present study were for four Leica 1200 GPS receivers respectively in July-August ('summer') 2007 and March ('winter') 2008.

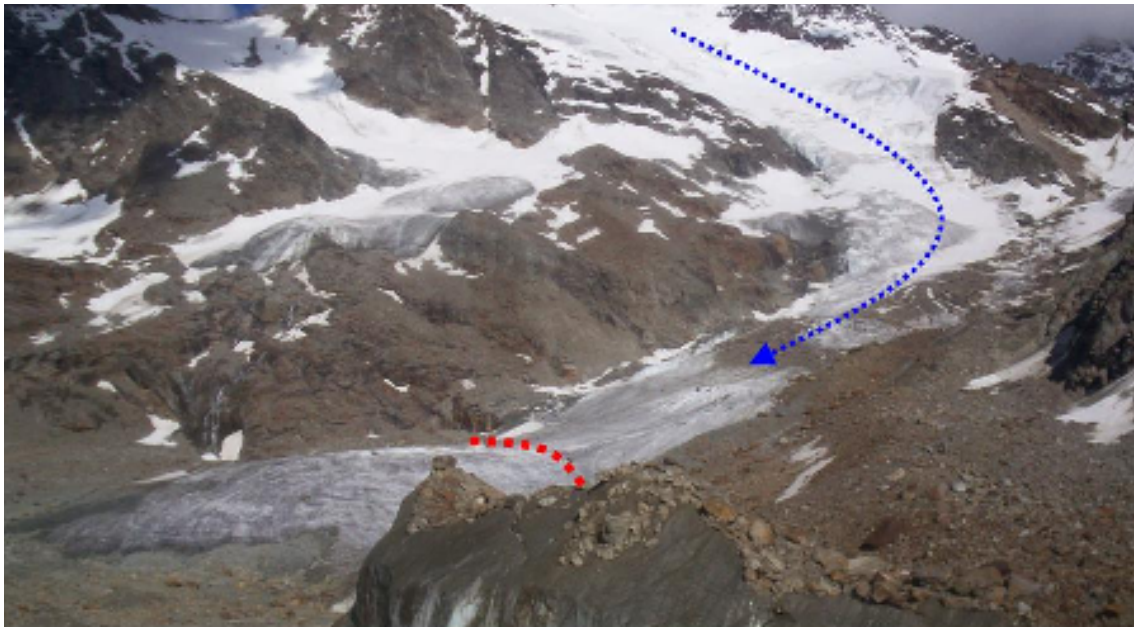

Figure 1. *Photograph of the Grubengletscher, showing the main ice flow direction (blue dotted arrow) the prominent break in slope referred to in the text (red dotted line).*

2. Field Site and Methodology

The Grubengletscher is a small valley glacier situated in the Saas Valley in Valais, Switzerland (Figure 1). In the summer it is accessible by four-wheel drive along a dirt track that leads up to the glacier from the village of Saas Balen, while in the winter helicopter transport is necessary for access. In the lower ablation zone a prominent break in surface slope of the Grubengletscher occurs (Figure 1), which was anticipated to indicate exceptional dynamic and subglacial mechanical behaviour around and particularly immediately downflow

of it. Accordingly our scientific efforts focused on the area around this break in slope. Our general strategy involved repeat acquisition of seismic AVO data on the same profile (permanently fixed on the glacier for the entire survey period) every day during the last week of July and the first week of August 2007 ('summer'), accompanied by differential GPS monitoring at three surrounding locations on the glacier and occasional automated GPR monitoring surveys. The seismic AVO and differential GPS measurements were repeated in March 2008 ('winter') to allow seasonal comparison of the data, anticipating in particular that the March 2008 ('winter') data could serve as a relatively invariable dynamic 'control' for the dynamically relatively variable summer data.

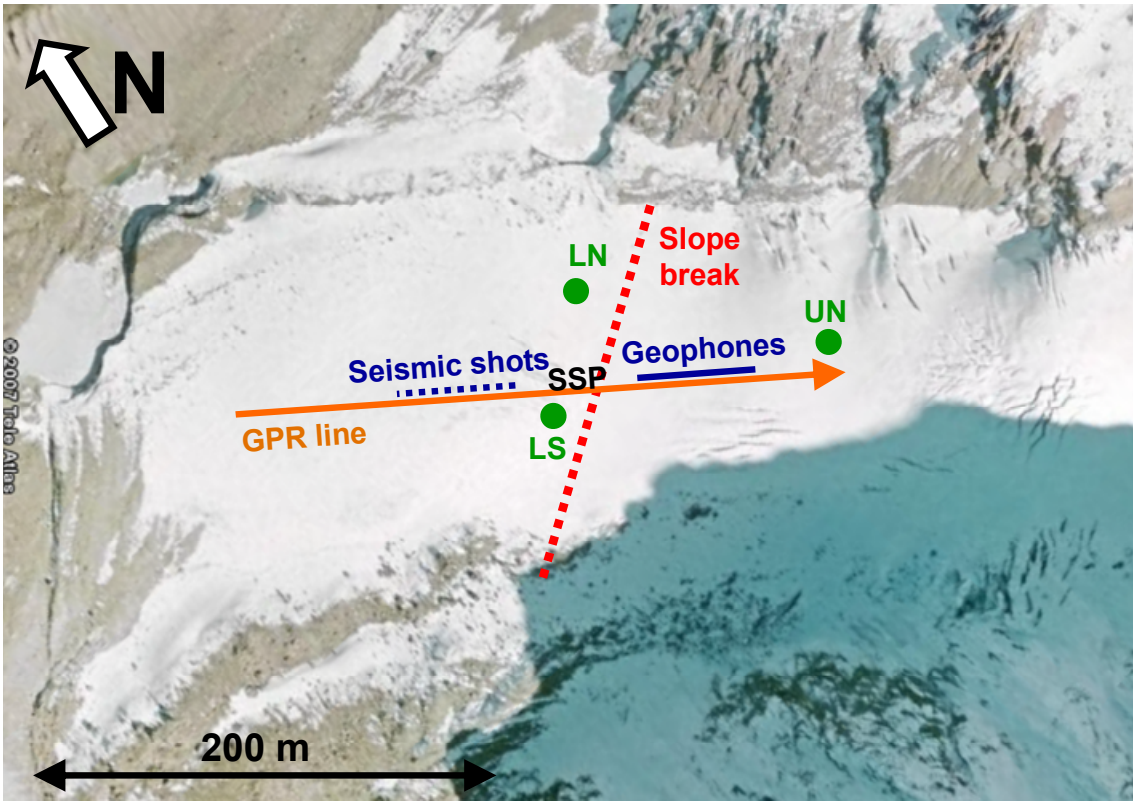

Figure 2. *Locations of GPS (green filled circles, station names as referred to in the text), seismic (solid blue line = geophone array; dotted blue line = seismic shot points; the 'seismic subglacial patch' (SSP) is located between the shots and the geophone array), and GPR (orange arrow, data collected from downglacier → upglacier), superimposed on a Google Earth image of the Grubengletscher. Ice flow is from right to left, and the GPS base station is located off to the left of the photograph on immobile sediments. The prominent break in slope is shown for reference. The Winter GPS station was located close to GPS station LS.*

2a. Seismic AVO measurements

Although a range of seismic experiments was conducted (including two common midpoint (CMP) 'supergathers' to infer the detailed seismic velocity structure of the glacier), the key experiment was an AVO experiment along a permanently-fixed 208.5 m long profile established longitudinally along the glacier centreline (Figures 2 and 3a). It used 48 28-Hz vertical geophones spaced 1.5 m apart in the upstream portion of the profile, generating a 70.5 long geophone array (0-70.5 m along the profile). Geophones were inserted directly into the ice and held in place by rocks in the summer; this avoided 'melting out' of geophones and undue loss of contacts with the ice as the geophones heated up during the day.

Notwithstanding, the geophones needed to be replanted regularly (at least once daily) in the summer. In the winter all geophones were buried at a spade's depth in the snow. The snow had variable thickness ranging between a few centimetres and more than a metre. Twelve shot points were established at 6 m spacing in the downflow portion of the seismic profile (Figure 2; 142.5-208.5 m along the profile), and a hammer-and-plate source was used to generate the seismic waves (Figure 3b). Two Geometrics 'Geode' seismographs were used to record the seismic data, which were stored and displayed on a Toughbook laptop computer; this allowed ongoing quality control of the data acquired as the surveys progressed. The geometrical arrangement of the seismic shot points and the geophone array was such that a 'seismic subglacial patch' (SSP) some 36 metres in diameter was the focus of the seismic investigations (Figure 2). The seismic AVO surveys were repeated every day between 25th July 2007 and 5th August 2007. A particularly comprehensive AVO data set (9 repeat sequences of all twelve shotpoints between ~ 0900 hrs and ~ 1900 hrs) was collected on August 1st, 2007, to elucidate in detail any possible subglacial hydrological-mechanical changes that occur on sub-daily timescales. It is this dataset that has produced the scientifically most interesting results, and will therefore be the focus of this report. All seismic data were analysed with the ReflexW software.

a **b**

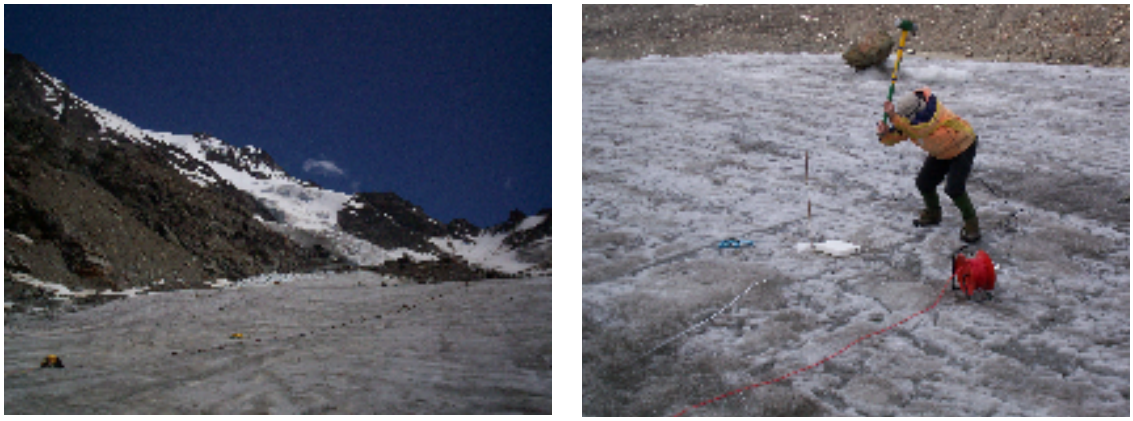

Figure 3. ***a:*** *Photograph of the permanently fixed geophone array on the steeper part of the survey area.* ***b:*** *Hammer-and-plate seismic source.*

2b. GPR

A Sensors and Software PE Pro GPR system (property of Swansea University) was used to map ice thicknesses and subglacial sedimentary strata in the study area (Figure 2), using the common-offset (CO) acquisition procedure (Figure 4a). We experimented with a range of antenna frequencies (50, 100 and 200 MHz), and found that the 50 MHz antennas gave the best results for our purposes. The CO surveys were accompanied by comprehensive CMP experiments to determine the detailed radar velocity structure of the glacier. In addition to the CO and CMP surveys we also set up the 50 MHz antennas within the SSP (Figure 2) to run continuously and autonomously between ~ 0840 hrs and 1840 hrs on August 1st, 2007 (Figure 4b), complementing the most comprehensive seismic data set (above). In this case the radar antennas were held in place by rocks (Figure 4b), which prevented them from sliding down the glacier. One radar trace was stored approximately every 10 minutes during the day, representing the stacked average of 4096 acquisitions at 0.8 ns sampling interval in each case. All GPR data were analysed with the ReflexW software, although the longest longitudinal GPR profile was later re-processed with ProMax. Processing of the monitoring data was limited to dewowing and static time shifts to avoid distortion of the reflection amplitudes and

phases. The constant-offset GPR data were additionally band-pass and median filtered as well as Kirchhoff-migrated and energy-decay corrected.

a **b**

Figure 4. ***a:*** *Constant-offset GPR survey.* ***b:*** *Automated GPR monitoring.*

2c. GPS

In both summer 2007 and winter 2008 one Leica 1200 GPS receiver was installed on non-moving sediments below the terminus of the Grubegletscher as a stationary GPS base station for our differential GPS surveys, secured by boulders and rocks (Figure 5a). In summer 2007, a second Leica 1200 GPS receiver was used initially to collect digital elevation data on the glacier surface (Figure 5b), including the elevations of the seismic and radar profiles. Subsequently three Leica 1200 GPS receivers were installed permanently on the glacier surface in the vicinity of the seismic profile, and particularly in the vicinity of the SSP (Figures 2 and 5c). Instead of mounting the GPS receivers on survey poles drilled into the ice, which experience shows tend to 'melt out' and tilt during the summer, we trialled a new mode of GPS receiver placement. Accordingly all three GPS receivers were placed on large boulders on the glacier surface, powered by standard car batteries that were constantly recharged by solar panels (Figure 5c). The most continuous differential GPS data set, for temporally coincident post-processing of glacier surface motion at the three locations, was obtained between July 27th and August 5th 2007. It is therefore this continuous record that our report will focus on, particularly with a view to consolidating the particularly comprehensive seismic and GPR data sets on August 1st, 2007.

We had originally planned a one-week long field deployment by helicopter in March 2008 to repeat the seismic AVO surveys as well as the GPS surveys at the three summer locations on the glacier (plus the GPS base station deployment in front of the glacier); however bad weather conditions grounding the helicopters eventually cut that deployment down to 1.5 days (March 26-27 2008). Due to these severe time limitations only the off-glacier Leica 1200 GPS base station and one Leica 1200 GPS receiver on the glacier (within the SSP) could be installed.

For the summer GPS data, three-dimensional ice displacement was determined at 15 s intervals with reference to the off-ice base station sited at the glacier front less than 1 km away using standard geodetic techniques[18]. Logged L1/L2/L2C data were post-processed under a kinematic solution using Leica GeoOffice proprietary software with precise ephemeris. Solutions with carrier cycle ambiguities were rejected along with solutions that yielded a vertical plus horizontal root-mean-square (rms) positional error of > 3 cm. For the winter GPS data, L1 and L2 phase solutions (with ambiguities rejected) were determined using the Trimble Business Centre Software using precise ephemeries. Here, solutions with an RMS Error of >0.01m (1cm) were rejected.

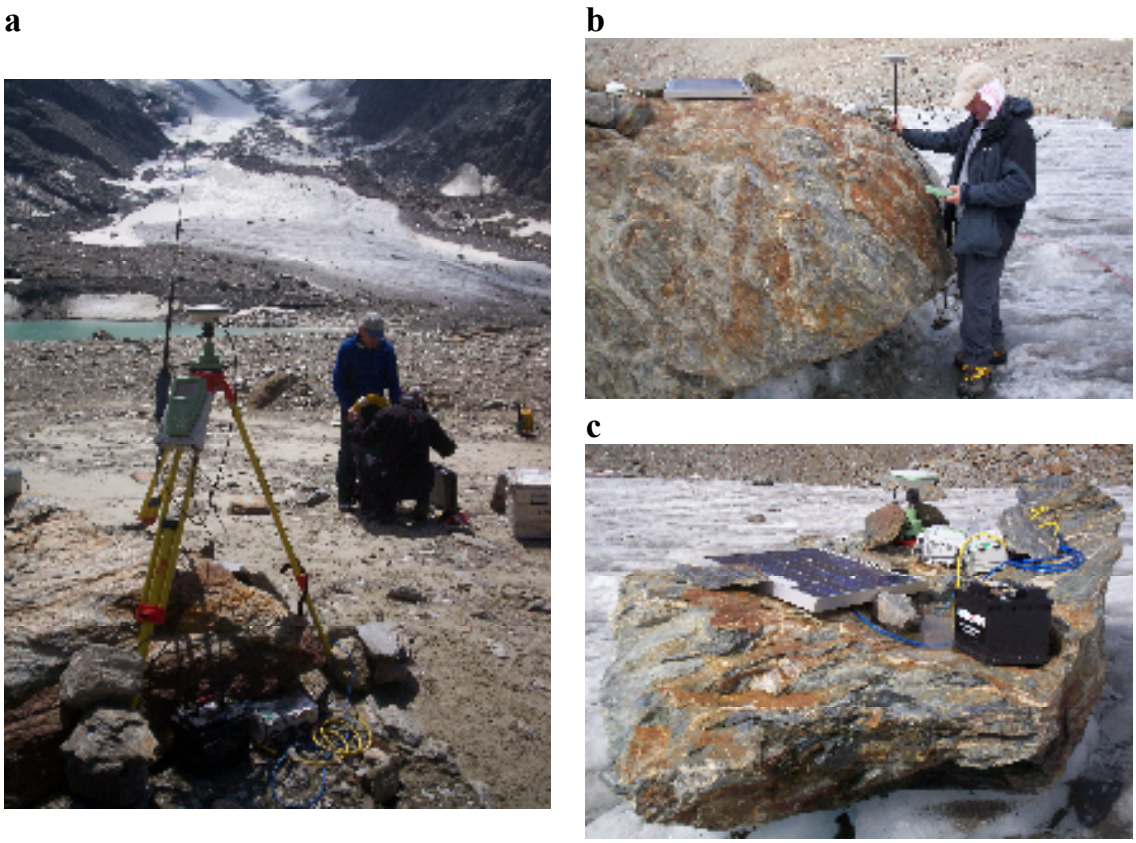

Figure 5. ***a:*** *GPS base station on immobile sediments in front of the glacier, secured by boulders and rocks.* ***b:*** *Collecting digital elevation data.* ***c:*** *GPS monitoring station installed on a boulder on the glacier.*

3. Results

3a. GPS data

In this study we are particularly interested in correlating changes in glacier flow velocity and glacier surface elevation with coupled hydrological-mechanical processes at the glacier bed; thus we present the differential GPS data from the three on-glacier monitoring stations in these terms. We found that the mean horizontal (mean vertical) velocities of the stations UN, LS, and LN (see Figure 2 for map and key) were respectively 0.083 (-0.021) m day^{-1}, 0.096 (-0.028) m day^{-1} and 0.063 (-0.059) m day^{-1}. Since station UN is located in a much steeper part of the glacier (Figures 1 and 2) it is not surprising that it's mean vertical velocity is more than twice that of the other two stations. Station LN was located close to the northern margin of the glacier tongue, which could explain why this sector of the glacier has a horizontal velocity that is noticeably slower than the more centrally located sectors (i.e. closer the glacier centreline) on which stations UN and LS were located (Figure 2).

Hourly-averaged differential GPS data from the three stations for the temporally most continuous and coincident period of 27 July to 5 August 2007 are shown in Figure 6a. It is readily apparent that all three stations show consistent and persistent diurnal cycles in horizontal velocities (lower panel in Figure 6a). More specifically, the sectors of the glacier monitored by GPS all accelerate in mid to late afternoon, and are characterised by maximum flow velocities late in the afternoon or early in the evening and minimum flow velocity in early to mid morning. The peak-to-peak amplitudes of the diurnal velocity cycles are more pronounced for stations UN and LS compared to station LN, which confirms the earlier

inference that station LN was located further away from the main axis of glacier flow compared to stations UN and LS. Compared to the compelling diurnal cycles in horizontal velocities it is challenging to identify statistically significant, consistent changes in the vertical velocities (upper panel in Figure 6a).

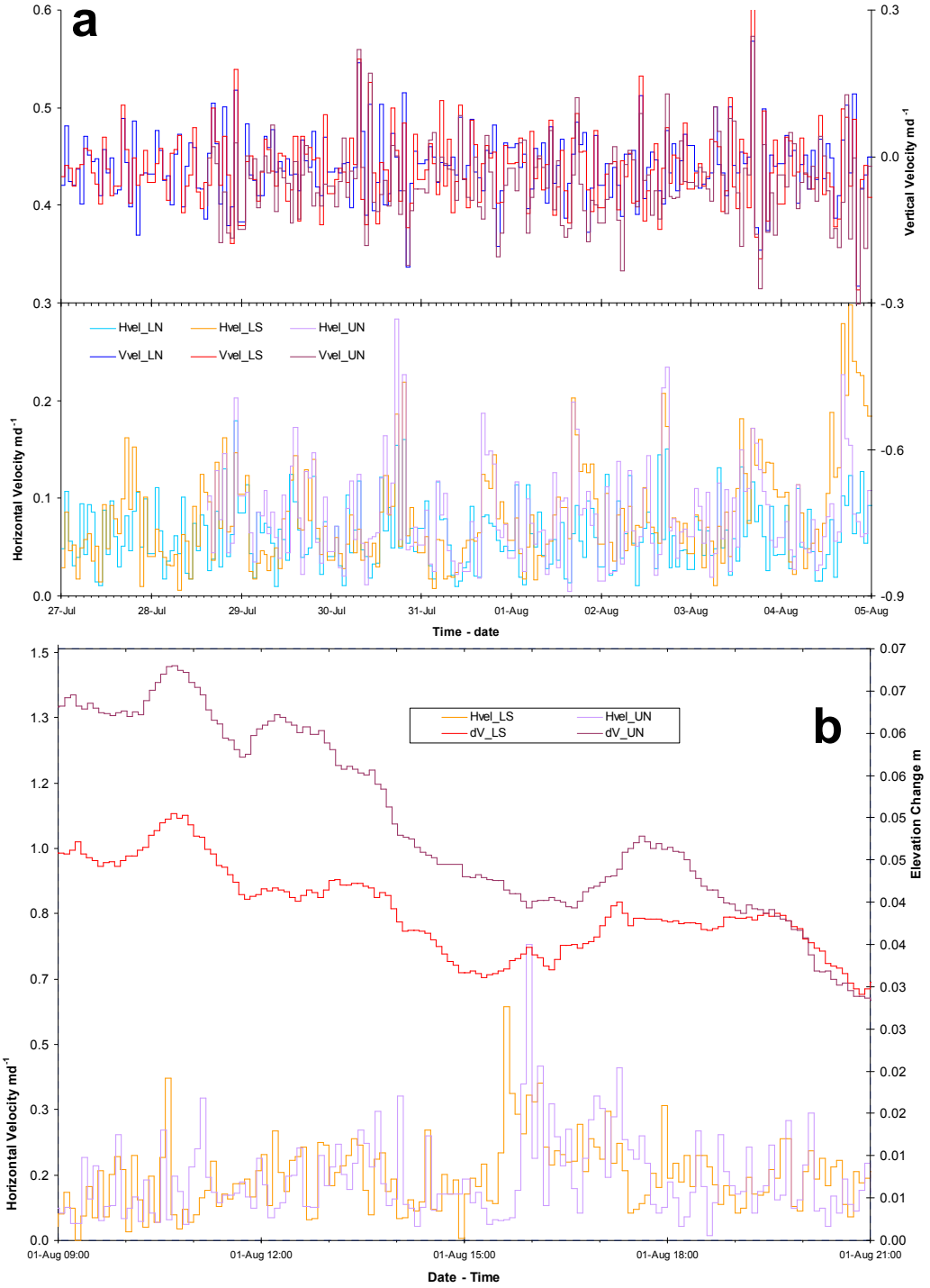

Figure 6. ***a:*** *Hourly averaged vertical (upper panel) and horizontal (lower panel) velocities at our three GPS stations for the period 27 July to 5 August 2007.* ***b:*** *Horizontal velocities and elevation changes of stations UN and LS on August 1st 2007, averaged over 5 minutes.*

Hourly-averaged differential GPS data from the three stations for the temporally most continuous and coincident period of 27 July to 5 August 2007 are shown in Figure 6a. It is readily apparent that all three stations show consistent and persistent diurnal cycles in horizontal velocities (lower panel in Figure 6a). More specifically, the sectors of the glacier monitored by GPS all accelerate in mid to late afternoon, and are characterised by maximum flow velocities late in the afternoon or early in the evening and minimum flow velocity in early to mid morning. The peak-to-peak amplitudes of the diurnal velocity cycles are more pronounced for stations UN and LS compared to station LN, which confirms the earlier inference that station LN was located further away from the main axis of glacier flow compared to stations UN and LS. Compared to the compelling diurnal cycles in horizontal velocities it is challenging to identify statistically significant, consistent changes in the vertical velocities (upper panel in Figure 6a).

As reflected well in the elevation changes for August 1st, 2007, averaged over five minutes (Figure 6b), glacier surface motion is principally downhill during the day for stations UN and LS (as the two most representative stations of near-centreline motion processes), as can reasonably be expected. However, during mid to late afternoon compelling and persistent anomalous rises in surface elevations are evident at both stations, which coincide temporally approximately with the aforementioned horizontal speed-ups (here averaged over five minutes, as opposed to the hourly averages for these stations in Figure 6a). It is particularly interesting to note that both glacier surface acceleration and surface rise at station UN lags temporally behind station LS by about 20 minutes. These implies that the dynamic processes governing the observed changes in glacier surface speed and elevation appear to affect the lower sector of our survey area before its upper sector.

The winter GPS data serve can serve as a control for the summer GPS data recorded (Figure 6c). Here, vertical displacements are negligible within the statistical error during the period monitored. Horizontal displacement is ~ 0.01 m day^{-1} during the 24-hour period monitored, and thus considerably smaller than displacements measured in the 2007 summer.

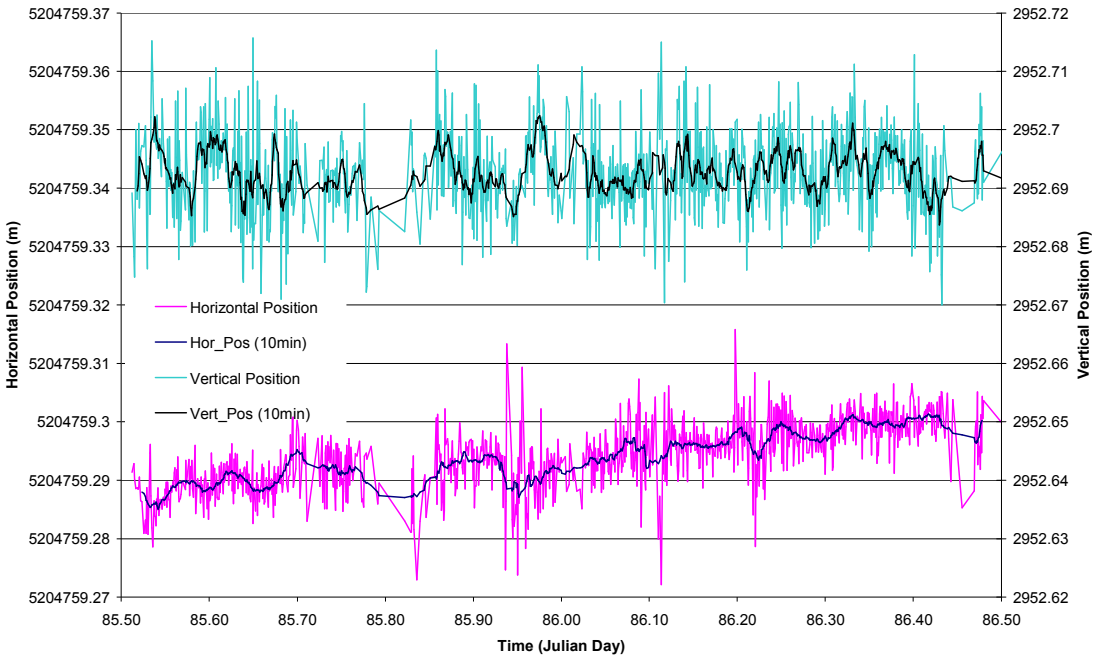

Figure 6 (continued). ***c:*** *Horizontal and vertical positions of the winter GPS station (located close to summer station LS; cf. Figure 2) between 26-27 March, 2008 (Julian days 85-86).*

3b. GPR data

The principal 'long' radargram acquired sub-parallel to glacier flow is shown in Figure 7a (cf. Figure 2 for profile location). The glacier bed reflector is readily apparent in the lower and middle sections of our survey area, as are sub-bed structures within our SSP (Figures 7a and 7b). Numerous englacial scatterers of radar energy are apparent in these sections, although it is challenging to identify any consistent patterns in their spatial distribution. The bed reflector is less well pronounced in the upper section of our survey area, and indeed particularly chaotic where a sharp increase in bed elevation occurs immediately upstream of our 'seismic subglacial patch' (Figure 7a). Two dominant reflectors successive in two-way travel time appear in the extreme upper section (Figure 7a). Encouragingly the base of the ice in our SSP is flat and horizontal (Figure 7b), which is also the case orthogonal to ice flow (as evident from our cross-GPR lines; not shown here). This facilitates ease of data analysis (for example with respect to correcting seismic and radar data for basal reflector dip), and significantly reduces the impact of 'side-swipe' from the surrounding valley walls on our data.

Our analyses of the continuous GPR data acquired autonomously on August 1st have already been published[19]. They are not repeated here since this report focuses on the GPS data gained from the instruments on loan from GEF. The key result from these GPR analyses was the inference that subglacial radar reflectivity increases strongly at 1500 hrs on that day, which is consistent with the arrival of significant quantities of melt water within the SSP at that time.

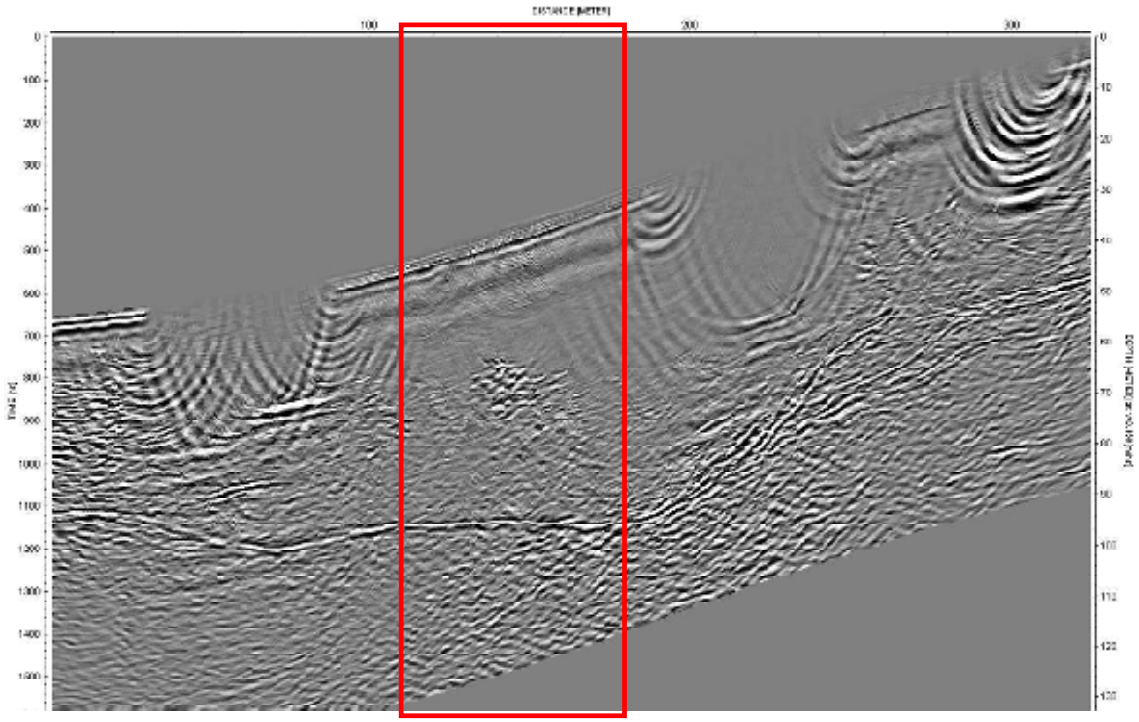

Figure 7. ***a:*** *'Long' GPR line acquired along the approximate axis of flow (cf. profile location in Figure 2). Ice flow is from right to left. Note that 'migration smiles' have not been edited out. The location of our 'seismic subglacial patch' (SSP) is indicated by the red box.*

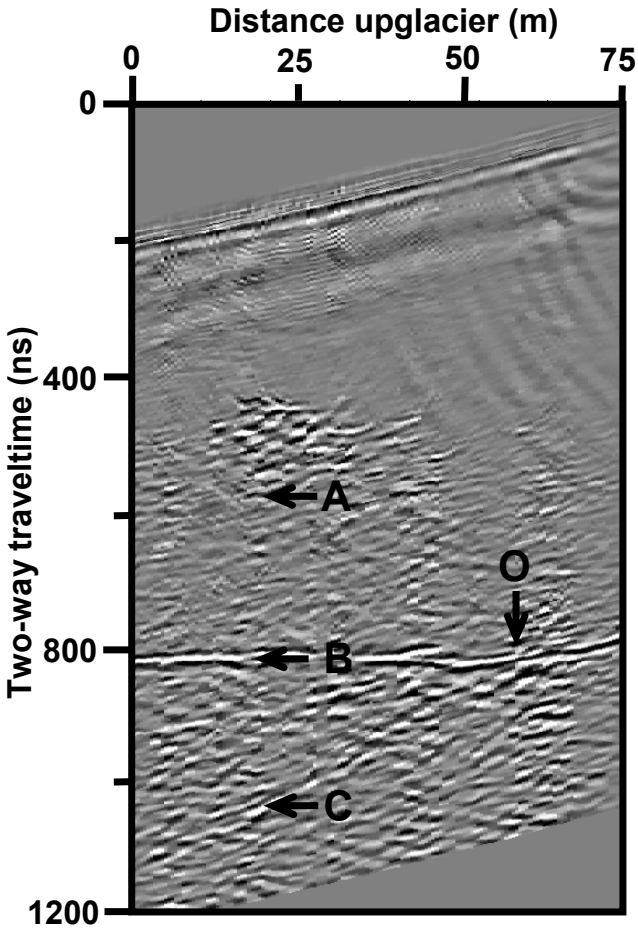

Figure 7 (continued). b: *SSP illustrating inferred englacial (A), ice-sediment (B) and sediment-bedrock (C) reflectors. The inferred sediment wedge thickens downglacier from its onset (O).*

3c. Seismic AVO data

Owing to the focus on the GPS data obtained from the GEF instruments, a detailed description of the seismic data analyses is also beyond the scope of this report. Suffice it to say here that the processed seismic CMP supergathers confirmed the sub-bed structures seen in the GPR data of our SSP (Figure 7b). We interpret the sub-bed radar and seismic reflectors as the base of a layer of unlithified subglacial sediments, and as an internal sediment horizon. It appears that the sediment layer originates near the upstream end of the SSP and thickens rapidly downstream (Figure 7b). In order to elucidate potential temporal changes in subglacial AVO reflectivity, the following processing stages were applied to the seismic shotgathers acquired at the nine different times (henceforth referred to as 'AVO sequences') on August 1st, 2007 (cf. Section 2a):

1. In each shotgather, the maximum half-cycle amplitudes of the direct wave and the basal reflector were picked.
2. In each shotgather, the basal reflector amplitude was normalised by that of the corresponding direct wave to eliminate changes in energy input into the ground caused by the hammer-and-plate source.
3. The normalised basal reflector amplitudes computed for each of the twelve shotgathers in any particular AVO sequence were averaged across the SSP.
4. The normalised and averaged basal reflector amplitudes from all nine AVO sequences were jointly plotted against theoretical incidence angle on the SSP, as shown in Figure 8a.
5. The maximum and mean normalised and averaged basal reflector amplitudes were calculated for each individual AVO sequence, and jointly plotted again time of acquisition, as shown in Figure 8b.

It is readily apparent from Figure 8a that maximum AVO reflectivity within the SSP occurs at incidence angles of ~ 41-42º. A rapid drop in reflectivity occurs at smaller incidence angles and an initially rapid but later less pronounced drop in reflectivity occurs at larger incidence angles. Significantly for the present study, both maximum and average AVO reflectivity varies consistently during the day on August 1st (Figure 8b); lower AVO reflectivity is inferred for the morning and late afternoon to early evening, and increasing and maximum AVO reflectivity is inferred for early to mid afternoon.

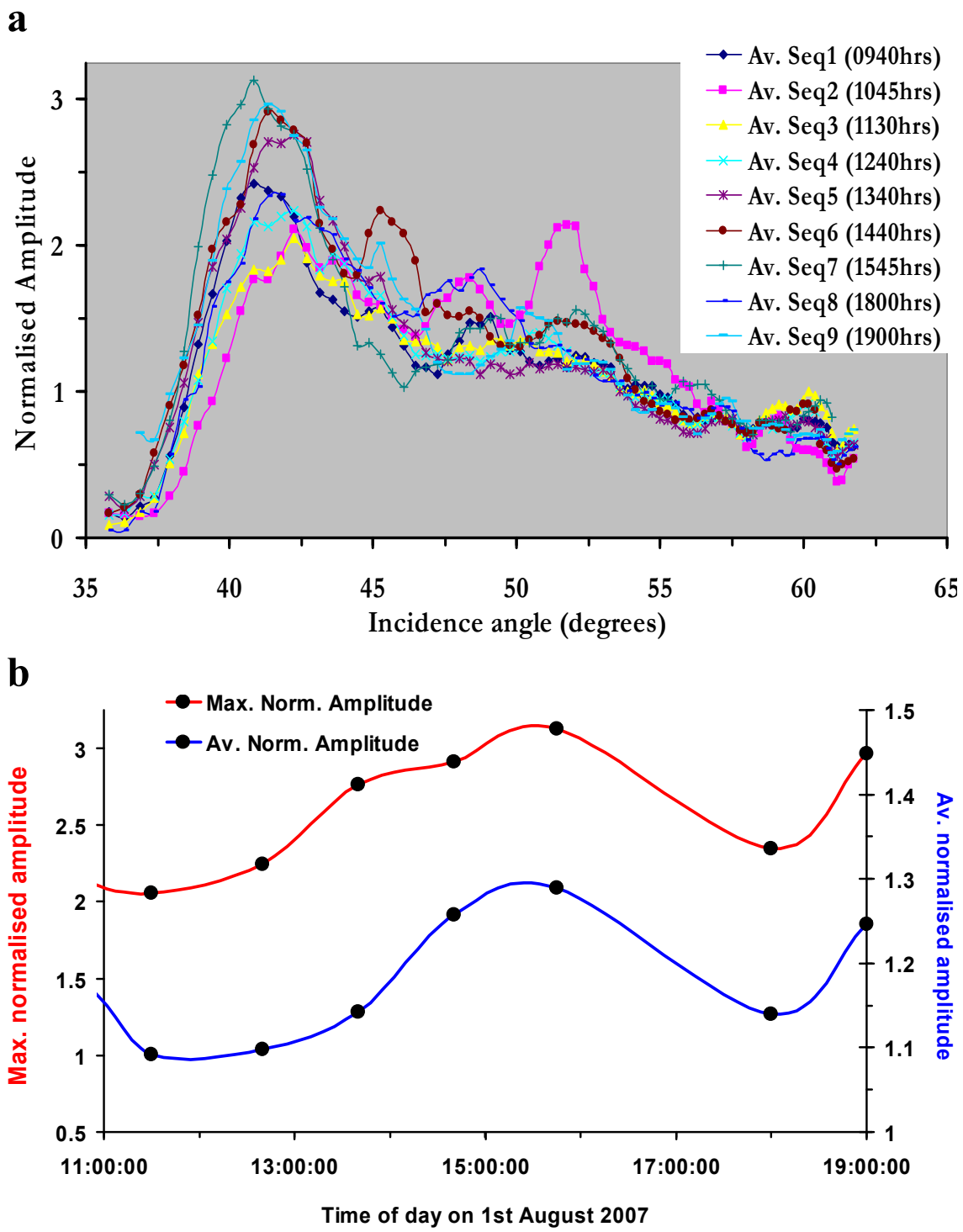

Figure 8. *Analyses of seismic AVO data.* ***a:*** *Normalised and averaged basal reflector amplitudes plotted against theoretical incidence angle on the SSP (as explained in the text). b: Diurnal changes in maximum and mean basal reflector amplitudes (normalised and averaged as in 'a' and as explained in the text) on August 1st, 2007.*

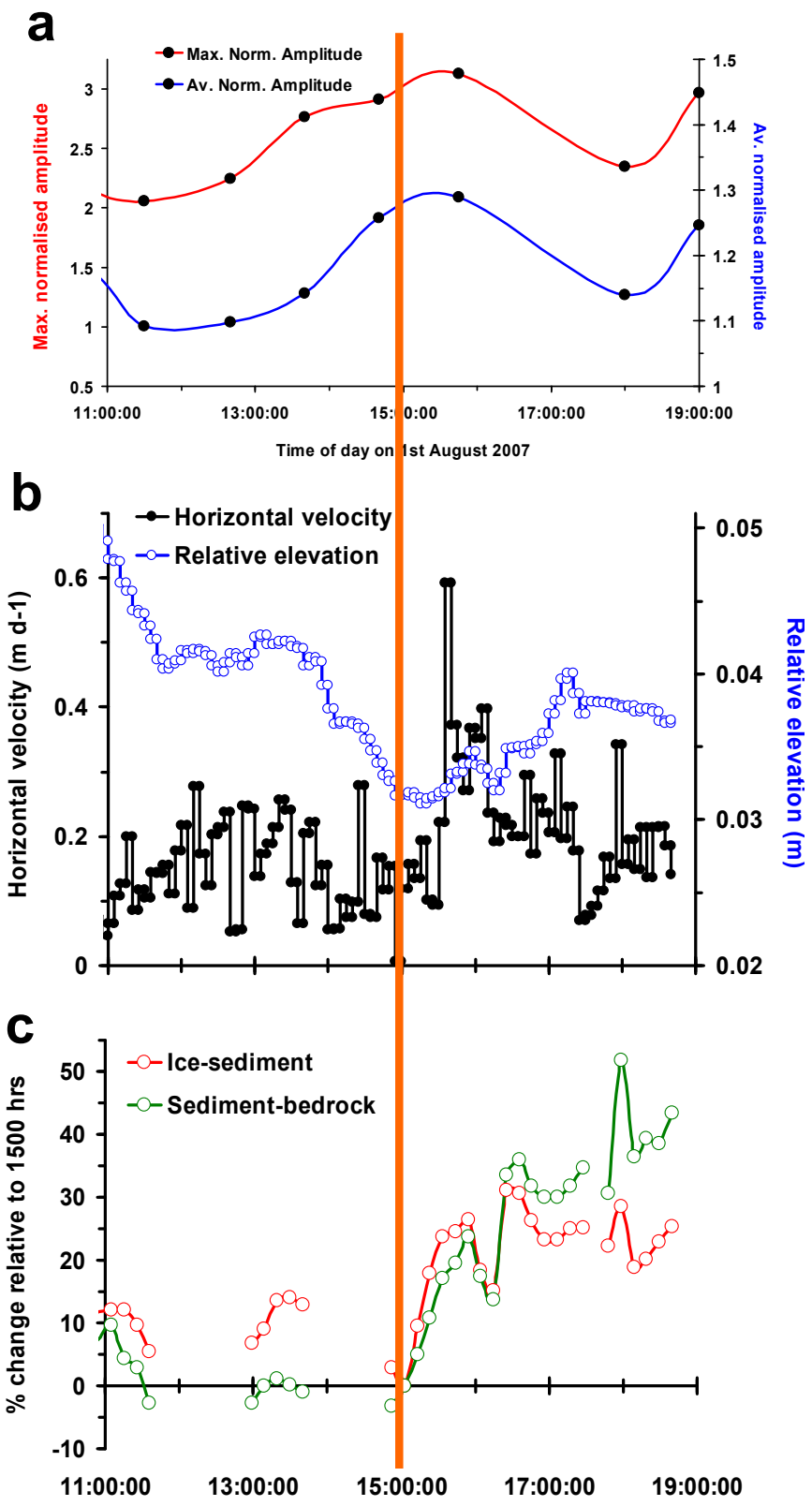

Figure 9. *Joint interpretation of seismic AVO (a) (cf. Figure 8b), horizontal velocities and relative elevations for GPS station LS (b) (cf. Figure 6b), and normalised radar amplitudes for the ice-sediment and sediment-bedrock reflectors (cf. Figure 7b).*

4. Joint Interpretation of GPS, seismic, and GPR data on August 1st, 2007

In elucidating the coupled hydrological-mechanical processes operating within the SSP, it is particularly instructive to interpret jointly the results from our GPS station LS which was located within the SSP (elevation change and horizontal velocity; Figure 9b), GPR (amplitudes of the ice-sediment and sediment-bedrock reflectors; Figure 9c (cf. Figure 7b)) and seismic AVO (temporal changes in maximum or average AVO reflectivity; Figure 9a). Before about 1500 hrs the glacier surface is lowering persistently and horizontal velocity is relatively slow and does not any statistically significant variations (Figure 9b). During this time radar reflectivity is relatively small (Figure 9c) and seismic AVO reflectivity is increasing steadily (Figure 9a); this increase implies that the sediments are progressively becoming acoustically softer. Together our observations are consistent with basal motion principally by sediment deformation during this time. We can speculate that basal shear stress increases as the glacier moves downhill with gravity at relatively low (or falling) subglacial water pressure (as indicated by persistent lowering of the glacier surface and low radar reflectivity), which leads to the observed steady increase in AVO reflectivity.

The significant enhancement of subglacial radar reflectivity later in the afternoon (Figure 9c) infers a persistent increase in the dielectric permittivity of the subglacial sediments that commences at 1430 h (preceded by an englacial transient in radar reflectivity that coincides temporally with a maximum modelled ablation rate of 19 cm d^{-1} equivalent[19]). Shortly after the englacial transient in radar reflectivity attenuates and the permittivity increase is initiated, the glacier surface experiences a significant and persistent uplift that commences at 1520 h (Figure 9b). Some 15 minutes thereafter a dramatic transient increase in the glacier's horizontal velocity occurs that rapidly reaches the highest values of horizontal velocity observed during the day (Figure 9b). At the same time seismic AVO reflectivity drops dramatically (Figure 9c), although the requirement for manual acquisition of the seismic data implies that temporal resolution is unfortunately not good enough to infer how rapid the decrease in AVO reflectivity is; or indeed at what precise moment in time this drop is initiated. We interpret this sequence of events as indicative of rising subglacial water pressures, supported by englacially routed delivery of surface melt waters that we may have witnessed[19], that eventually jack the glacier off the bed initiating a pronounced sliding event as the glacier is decoupled from the bed[20]). Rising, rather than high, subglacial water pressures appear to be a prerequisite for sliding in this case. This event terminates about half an hour later (~ 1610 h; Figure 9b), coincident with a transient drop in surface elevation (Figure 9b) and preceded by a transient decrease in the gradient of subglacial radar reflectivity (Figure 9c). As indicated by comparison of the GPS data from stations LS and UN (cf. Section 3a), it appears that the hydrologically-induced sliding event is initiated on the glacier tongue below the prominent break in surface slope (cf. Figures 1 and 2), and subsequently propagates upglacier.

Closer inspection of the relative variability of the two normalised subglacial radar reflections in Figure 9c reveals [i] larger amplitudes at the ice-sediment interface through the morning and the early afternoon; [ii] comparable amplitudes between 1430 h and 1620 h; and [iii] larger amplitudes at the sediment-bedrock interface from 1620 h onwards. Following from [i] it appears that the hydromechanical changes that give rise to the corresponding increases in sediment dielectric permittivity are relatively concentrated at or near the ice-sediment interface prior to and during the speed-up event. There is a remarkable temporal coincidence between the termination of this event and the instance at which the sediment-bedrock amplitudes become larger than the ice-sediment amplitudes (~ 1620 h; Figure 9c). The means of the subglacial radar reflections level off for a approximately hour after 1620 h, and then increase further as does the difference in reflectivity between the two subglacial

reflectors. Since there is no marked decrease in the reflectivity of the ice-sediment interface it is unlikely that the sediment-bedrock reflector becomes dominant since more energy is suddenly transmitted through this interface. It rather appears that the area of water-filled pore space exposed to the radar energy deeper within the sediments begins to increase during the pronounced sliding event. In absence of direct subglacial observations we cannot unfortunately elucidate whether increased exposure is caused by an increase in water content deeper within the sediments or some mechanical change within them.

Conclusions

We believe that our study demonstrates that temporally coincident collection and joint interpretation of high-quality differential GPS, repeat seismic AVO and continuous GPR data is well suited to addressing the principal aim of the present study; and more generally that our study demonstrates that such an integrated geophysical approach is well suited not only to characterising at a snapshot in time coupled hydrological and mechanical properties of the glacier bed, but also to monitoring changes in those properties over time. From this fundamental glaciological processes can be inferred, which may well hold true at outlet glaciers from Polar ice masses as they do for the Grubengletscher as a possible analogue. We thus conclude that basal motion of the Grubengletscher occurs principally by subglacial sediment deformation during much of the day, although hydrologically-induced sliding events are common, especially in afternoon as the glacier is decoupled from the bed (addressing specific objective SO1). The highest glacier flow velocities occur during these sliding events, as opposed to velocities that are relatively small and steady during times of sediment deformation (addressing SO2). It is readily apparent from our findings that hydrological processes are a governing control on basal mechanical processes at the Grubengletscher (addressing SO3).

Although data records are short due to bad weather (Section 2c), the GPS and seismic AVO data collected during the 1.5 day period in March 2008 provide an important control on the summer data. Specifically, a consistent diurnal change in glacier flow velocity or surface elevation change is not observed during this winter period. The winter seismic data are yet to be analysed, but we expect that any such changes will also be absent in these seismic data.

Future work will include AVO-based rock physics modelling (to be completed over the 2009 summer) to quantify the inferred changes in AVO reflectivity on August 1st in terms of the sediment mechanical and hydrological properties, which is anticipated to shed further light on the hydromechanical processes that occurred on that day. Our study is encouraging in that it demonstrates that surface geophysical measurements alone can infer fundamentally important subglacial properties and processes, to some extent reducing the need for borehole drilling and direct measurement at the glacier bed (such measurements were not logistically feasible in the present case due to budgetary constraints). Notwithstanding, borehole measurements would have the capacity to 'ground-truth' the geophysically-based inferences.

Acknowledgements

This study was supported by a Royal Society Research Grant (2006/R2) and two consecutive loans of four Leica 1200 GPS receivers (846 and 866), which are gratefully acknowledged. Bernd Kulessa would also like to thank Alan Hobbs (NERC-GEFE), Graham Stuart (University of Leeds), Adam Booth and Adrian Luckman (Swansea University), Alun Hubbard (Aberystwyth University) and Alex Brisbourne (NERC-SeisUK) for help in

acquiring and processing of the GPS, seismic and radar data, which would not have been possible without them; their efforts are highly appreciated and gratefully acknowledged.

References

1. Church J.A. & 7 others, In: J.T. Houghton & 7 others (eds), Climate change 2001: the scientific basis, IPCC, *Cambridge University Press*, 639, 2001. **2.** Alley R.B. & 3 others, *Science* (310) 456, 2005. **3.** Dowdeswell J.A., *Science* (311) 963, 2006. **4.** Oerlemans J. & 8 others, *Ann. Glaciol.* (42) 230, 2005. **5.** Zwally H.J. & 5 others, *Science* (297) 218, 2002. **6.** Boon S. & M. Sharp, *Geophys. Res. Lett.* (30) doi:10.1029/2003GL018034, 2003. **7.** Bingham R. & 2 others, *Ann. Glaciol.* (37) 181, 2003. **8.** Parizek B.R. & R.B. Alley, *Quat. Sci. Rev.* (23) 1013, 2004. **9.** Haeberli W. & 3 others, *J. Glaciol.* (47) 111, 2001. **10.** Haeberli W. & W. Fisch, *J. Glaciol.* (30) 373, 1984. **11.** Luckman A. & 3 others, *Geophys. Res. Lett.* (33) doi:10.1029/2005GL025428, 2006. **12.** Rignot E. & P. Kanagaratnam, *Science* (311) 986, 2006. **13.** Huybrechts P. & 3 others, *Global Planet. Change* (42) 83, 2004. **14.** Rott H. & 3 others, *Ann. Glaciol.* (34) 277, 2002. **15.** De Angelis H. & P. Skvarca, *Science* (299) 1560, 2003. **16.** Rignot E. & 5 others, *Geophys. Res. Lett.* (31) doi:10.1029/2004GL020697, 2004. **17.** Scambos T.A. & 3 others, *Geophys. Res. Lett.* (31) doi:10.1029/2004GL020670, 2004. **18.** King, M., *J. Glaciol.* (50) 601, 2004. **19.** Kulessa, B. & 3 others, *Geophys. Res. Lett.* (35) doi:10.1029/2008GL035855. **20.** Anderson, R. S. & 6 others, *J. Geophys. Res.* (109) doi:10.1029/2004JF000120.